CrossMark

ORIGINAL ARTICLE

Comparison of Enzymatic Hydrolysis and Acid Hydrolysis of Sterol Glycosides from Foods Rich in Δ^7-Sterols

Linda H. Münger[1] · Sabrina Jutzi[1] · Anna-Maija Lampi[2] · Laura Nyström[1]

Abstract In this study, we present the difference in sterol composition of extracted steryl glycosides (SG) hydrolyzed by either enzymatic or acid hydrolysis. SG were analyzed from foods belonging to the plant families *Cucurbitaceae* (melon and pumpkin seeds) and *Amaranthaceae* (amaranth and beetroot), both of which are dominated by Δ^7-sterols. Released sterols were quantified by gas chromatography with a flame ionization detector (GC-FID) and identified using gas chromatography/mass spectrometry (GC–MS). All Δ^7-sterols identified (Δ^7-stigmastenyl, spinasteryl, Δ^7-campesteryl, Δ^7-avenasteryl, poriferasta-7,25-dienyl and poriferasta-7,22,25-trienyl glucoside) underwent isomerization under acidic conditions and high temperature. Sterols with an ethylidene or methylidene side chain were found to form multiple artifacts. The artifact sterols coeluted with residues of incompletely isomerized Δ^7-sterols, or Δ^5-sterols if present, and could be identified as $\Delta^{8(14)}$-sterols on the basis of relative retention time, and their MS spectra as trimethylsilyl (TMS) and acetate derivatives. For instance, SG from melon were composed of 66 % Δ^7-stigmastenol when enzymatic hydrolysis was performed, whereas with acid hydrolysis only 8 % of Δ^7-stigmastenol was determined. The artifact of Δ^7-stigmastenol coeluted with residual non-isomerized spinasterol, demonstrating the high risk of misinterpretation of compositional data obtained after acid hydrolysis. Therefore, the accurate composition of SG from foods containing sterols with a double bond at C-7 can only be obtained by enzymatic hydrolysis or by direct analysis of the intact SG.

Abbreviations

ASG	Acylated steryl glycosides
DHC	Dihydrocholesterol
IS	Internal standard
FS	Free sterols
GC–MS	Gas chromatography/mass spectrometry
M	Molecular ion
m/z	Mass-to-charge ratio
ROH	Hydroxyl function of sterol derivative
SC	Side chain
SE	Steryl esters
SG	Steryl glycosides
TMS	Trimethylsilyl

✉ Laura Nyström
laura.nystroem@hest.ethz.ch

[1] Institute of Food, Nutrition and Health, ETH Zurich, Schmelzbergstrasse 9, 8092 Zurich, Switzerland

[2] Department of Food and Environmental Sciences, University of Helsinki, P. O. Box 27, FIN-00014 Helsinki, Finland

Introduction

Phytosterols are steroid alcohols structurally similar to cholesterol that occur at various concentrations and in

Springer AOCS

different proportions in vascular plants. They mainly differ in the structure of the side chain with regards to length, degree of unsaturation, and stereochemistry, as well as in number and position of double bonds within the ring structure. Phytosterols not only comprises different species of free sterols (FS), but also conjugates, namely steryl esters (SE), steryl glycosides (SG) and acylated steryl glycosides (ASG). It is of high importance to know the sterol profile of foods, as different sterols can produce different spectra of bioactivities.

Health benefits have been attributed to FS and sterol conjugates from plants, when consumed regularly [1]. Most attention is given to their cholesterol-lowering activity. The intake of phytosterols through fortified foods and from a natural diet can decrease serum and low-density lipoprotein (LDL) cholesterol, thereby decreasing the risk of cardiovascular diseases [1–4]. Health claims about the ability of FS and their esters to reduce the risk of cardiovascular disease have been accepted by both the European Food Safety Authority (EFSA) and the US Food and Drug Administration (FDA) [5, 6]. Glycosylated sterols have been shown to reduce cholesterol absorption even though the glycosidic bond is not cleaved during digestion [7, 8]. Furthermore, health benefits, such as modulation of the immune system and reduction of prostate hyperplasia, have been attributed to SG [9–11].

Structure–activity relationships have been observed for sterols in general; thus, different sterol species can exert different degrees of biological activity. For instance, sitostanol appears to be more effective than sitosterol with regards to the hypocholesterolemic effect, which is based on the inhibitory action towards the absorption of cholesterol [12]. Structural features of sterols also play an important role in lipid biosynthesis and metabolism by specifically affecting enzyme activities, depending, for instance, on the degree of side chain unsaturation [13]. Hence, differences in bioactivity based on structural differences can also be expected within the group of glycosylated sterols. Therefore, it is crucial not only to evaluate sterol contents of foods, but also to determine the single species composition (sterol profile) of FS, SE, ASG and SG.

The most common approach for total sterol quantification and identification of single sterol species combines alkaline and acid hydrolysis prior to gas chromatographic analysis (GC) in order to include all sterol conjugates [1, 14–16]. The exclusion of acid hydrolysis may lead to a severe underestimation of the total sterol content, because in certain foods the content of glycosylated sterols can even exceed FS and SE content [17]. Alternatively, SG can be directly analyzed by GC as a trimethylsilyl ether of the intact compound, thereby avoiding acid-catalyzed isomerization [18–21]. As a drawback, this method depends on external calibration due to the lack of a

suitable internal standard, and complete derivatization of all hydroxyl groups remains a critical step. Daily phytosterol intakes [2, 22] and total sterol contents of foods [14, 17, 23–25], assessed by performing alkaline and acid hydrolysis, have focused on the quantification of the most abundant sterols in foods, such as sitosterol, campesterol, stigmasterol, and their stanols (all Δ^5-sterols), with the amounts of the less abundant sterol species often not reported.

Under acidic conditions and at elevated temperature, some sterols undergo acid-catalyzed isomerization and artifact sterols are produced [23, 26, 27]. As a result, the composition of sterols found after sample preparation does not reflect the correct sterol profile of the plant material. Δ^5-Avenasterol and its diastereomer, fucosterol, contain an ethylidene-side chain that is particularly sensitive to isomerization due to the formation of a carbenium ion at low pH [26]. Evidence was also presented that Δ^5-avenasteryl and Δ^7-avenasteryl glycoside are even decomposed under acid conditions [27].

In general, the composition of FS is reflective of the composition of glycosylated sterols; however, this relationship cannot be concluded in presence of labile sterols and if acid hydrolysis is employed. Plants from the families *Cucurbitaceae* and *Amaranthaceae* are dominated by Δ^7-sterols (Fig. 1) [23, 28–30]. In pumpkin seeds, Δ^7-steryl glucosides have been identified on the basis of liquid chromatographic methods and nuclear magnetic resonance (NMR) [28, 31]. Some Δ^7-sterols found in *Cucurbitaceae* have an additional unique structural feature: 24-ethyl sterols bearing a Δ^{25}-double bond are composed of (24S)-epimers (as e.g. in poriferasta-7,25-dienol, Fig. 1e) [32, 33]. As demonstrated by Phillips et al. 2005 [23], the analysis of pumpkin seed sterols showed that acid hydrolysis had a drastic impact on the resulting composition because several unknown artifact compounds were produced. In total sterol analysis, the authors showed that Δ^7-stigmastenol was only found if acid hydrolysis was omitted [23]. Thus, acid lability of Δ^7-sterols leading to isomerization or decomposition has been reported [23, 28], but has not yet been studied in detail due to the lack of alternative analytical procedures. Certain Δ^7-sterols (e.g. Δ^7-stigmastenol) occur in high proportion along with Δ^5-sterols; for instance, in plants from *Theaceae* and in sunflower seeds (*Asteraceae*) [34, 35],

As recently demonstrated, acid hydrolysis of SG can be replaced by enzymatic hydrolysis, which is a powerful tool to reveal correct sterol profiles of SG extracts from foods [36]. So far, enzymatic hydrolysis of SG has not been applied widely to foods from Δ^7-sterol-dominated plant families. The accurate percentage composition of the SG fraction is not yet known, since it contains several potentially acid sensitive sterols.
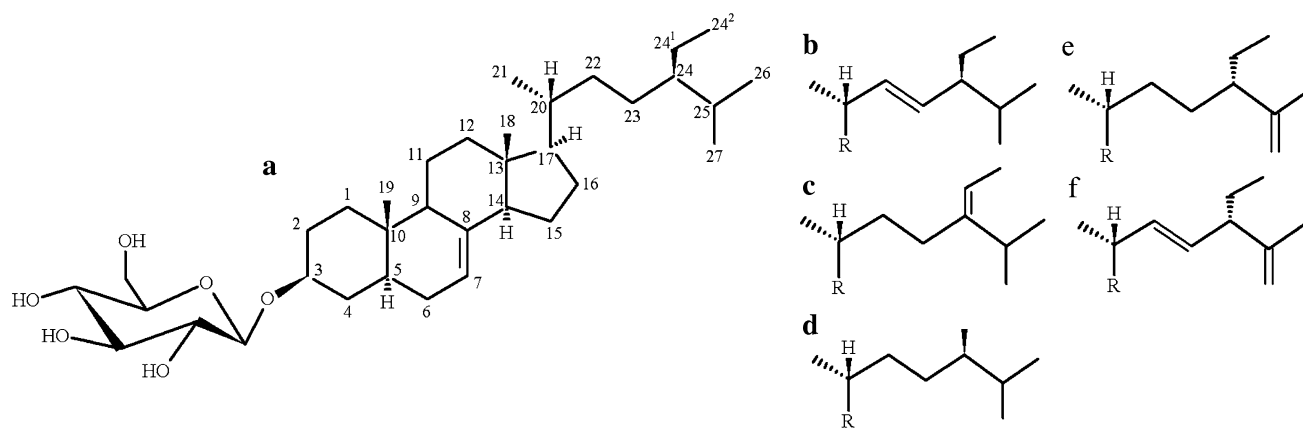
Fig. 1 a Molecular structure of Δ⁷-stigmastenyl glucoside [systematic name: (24R)-24-ethyl-5α-cholest-7-en-3β-yl-β-D-glucopyranoside] and side chains of other Δ⁷-sterol glucosides (systematic name of free sterol); **b** spinasteryl glucoside [(22E,24S)-24-ethyl-5α-cholesta-7,22-dien-3β-ol], **c** Δ⁷-avenasteryl glucoside [(24Z)-24-ethylidene-5α-cholest-7-en-3β-ol], **d** Δ⁷-campesteryl glucoside [(24R)-24-methyl-5α-cholest-7-en-3β-ol], **e** poriferasta-7,25-dienyl glucoside [(24S)-24-ethyl-5α-cholesta-7,25-dien-3β-ol] and **f**: poriferasta-7,22,25-trienyl glucoside [(22E,24R)-24-ethyl-5α-cholesta-7,22,25-trien-3β-ol]

Therefore, the aim of this study was to evaluate the impact of acid hydrolysis on SG from foods dominated by Δ⁷-sterols, based on comparison to enzymatically hydrolyzed SG fractions. Comparison of these two hydrolysis procedures allowed for the identification of labile sterols, and identification and structural elucidation of artifact peaks after acid hydrolysis. Moreover, the correct percentage composition of the SG fraction of the enzymatically treated samples was revealed.

Materials and Methods

Reagents

A commercially available SG mixture, denoted as SG standard in this study (total SG: >98 %, approx. 56 % sitosteryl glucoside, 25 % campesteryl glucoside, 18 % stigmasteryl glucoside, and 1 % Δ⁵-avenasteryl glucoside), was obtained from Matreya Inc. (Pleasant Gap, USA). Acetone (≥99.5 %), isopropanol (≥99.9 %), ethanol (≥99.8 %), diethyl ether (≥99.8 %), anhydrous pyridine (≥99.8 %), cyclohexane (99.7 %), hydrochloric acid (HCl, 37 %), potassium hydroxide (KOH, pellets, ≥86 %), anhydrous sodium acetate (≥99.0 %), acetic acid (100 %), dihydrocholesterol (DHC, 5α-cholestan-3β-ol, ca. 95 %), trimethylchlorosilane (TMCA, GC grade), and N,O-bis(trimethylsilyl)trifluoroacetamide (BSTFA, GC grade) were purchased from Sigma (Buchs, Switzerland). Hexane (96 %) was obtained from Scharlau (Barcelona, Spain), acetic anhydride (p.a.) from Merck (Darmstadt, Germany), and dichloromethane (99.99 %) from Fisher Scientific (Loughborough, UK). All solutions were prepared with Milli-Q® purified water using a Merck Millipore purification system. For the enzymatic hydrolysis of SG, Fructozyme® L (liquid mixture of exo- and endoinulinases from Aspergillus niger, EC 3.2.1.80 and EC 3.2.1.7, Novozymes A/S, Bagsvaerd, Denmark) was used, for which hydrolytic activity on SG has been evaluated elsewhere [36].

Sample Preparation—Lipid Extraction and Fractionation

All food samples were bought in local groceries stores and were prepared in triplicate (from one food product, three samples were prepared). The moisture content of food samples was determined in duplicate by the gravimetric method after drying at 104 °C overnight. The flesh of melon (Cucumis melo reticulatus, Galia) and beetroot without peel (Beta vulgaris) were first freeze-dried and then ground, whereas raw seeds from pumpkin (Cucurbita pepo) and grains from amaranth (Amaranthus caudatus) were directly ground to a fine powder using a Grindomix GM200 mill (Retsch, Haan, Germany). Two grams of each dry sample were subjected to accelerated extraction using acetone as solvent for lipid extraction (ASE 350 Dionex, Thermo Fisher Scientific, Reinach, Switzerland). Isolates used for further enzymatic or acid hydrolysis were prepared separately. The acetone extracts were evaporated to dryness under vacuum and redissolved in 2.5 ml hexane:isopropanol 95:5. Lipids were fractionated by solid phase extraction (SPE) using diol cartridges (GLScience, InertSep®, 500 mg, 3 ml), based on a protocol published previously [17]. The last elution with hexane:isopropanol, which eluted SG from the column, was collected, and this fraction was dried under vacuum and subjected to

either acid or enzymatic hydrolysis. Furthermore, a pure SG standard solution was prepared at a concentration of 0.21 mg/ml in hexane:isopropanol 80:20. Pure SG standard samples (200 μg) were directly subjected to acid or enzymatic hydrolysis (in triplicate).

Acid Hydrolysis of SG

Following SPE, acid hydrolysis was performed based on the protocol published by Nyström et al. [17] with minor modifications. In short, the residues were redissolved in 2 ml ethanol and 1 ml of full fat milk was added, mimicking the food matrix. Acid hydrolysis was performed with 6 M HCl at 85 °C for 30 min. One ml of the internal standard (IS) solution (DHC, 0.016 mg/ml in ethanol) was added after acid hydrolysis but prior to extraction, in order to ensure comparability to the enzymatic hydrolysis procedure. For extracting released FS, 10 ml hexane-diethyl ether and 4.5 ml Milli-Q water were added and upper layer was collected. In order to remove residual saponifiable compounds originating from the milk that would impact GC analysis, alkaline hydrolysis was performed in 4 ml ethanol and 0.25 ml oversaturated KOH solution, as in [17]. The residues after evaporation were redissolved in 0.7 ml dichloromethane. For the determination of FS recovery, the pure SG standard (200 μg, in triplicate) was also subjected to the procedure above. Under the same conditions, an experiment using the SG standard but without addition of milk was performed.

Enzymatic Hydrolysis of SG

The protocol for enzymatic hydrolysis is based on Münger and Nyström [36]. Both the residues remaining after SPE and pure SG standard mixture (for determination of FS recovery) were redissolved in 500 μl ethanol and 2.8 ml 0.1 M sodium acetate buffer (pH 4.5). After mixing, 200 μl Fructozyme® L was added, and the incubation was performed at 40 °C in a shaking incubator for 18 h. Prior to the extraction, 1 ml of the IS solution (DHC, 0.016 mg/ml DHC in ethanol) was added to samples. The released FS were extracted by the addition of 10 ml hexane-diethyl ether and 7 ml Milli-Q water. Samples were mixed well, and if necessary, phase separation was enhanced by centrifugation. The top layer was collected, dried under vacuum, redissolved in 0.7 ml dichloromethane and transferred to a small glass vial.

Trimethylsilyl (TMS) Derivatization and Gas Chromatography with a Flame Ionization Detector (GC-FID) Analysis

All hydrolyzed samples underwent derivatization in order to produce trimethylsilyl (TMS) derivatives of the released

FS. Therefore, the dichloromethane solutions were dried under nitrogen stream at 50 °C and redissolved in 100 μl pyridine. TMS-derivatization was performed as in Nyström et al. [17]. After derivatization and drying, 200 μl hexane was added. Samples with high sterol concentration were further diluted ten times before analysis by gas chromatography with a flame ionization detector (GC-FID). GC analysis was based on the method in Nyström et al. [17] using a Trace GC 2000 gas chromatograph (ThermoQuest, CE Instruments) equipped with an autosampler, on column injector, RTX-5 fused-silica capillary column (diphenyl and dimethyl polysiloxane [5:95]; 60 m, 0.32 mm id, 0.1 mm film, Restek Corp., Bellefonte, PA, USA) and an FI detector. The quantification of the single sterol species as FS was based on the IS. The total SG amount/g DM was calculated based on the FS, quantified, and transformed by using a theoretical conversion factor of 1.39 (corresponds to molecular proportion of glucosylated sitosterol to free sitosterol).

Acetate Derivatisation

As more literature on GC–MS spectra is available for sterols as acetate derivatives than as TMS derivatives, acetate derivatisation was also applied on previously unidentified sterols for structural elucidation. After the evaporation of the solvents of the FS fractions under nitrogen at 50 °C, 100 μl acetic anhydride and 100 μl pyridine were added. Samples were acylated at 60 °C for 30 min. Samples were dried again and redissolved in 200 μl heptane and subjected to GC–MS analysis as described below.

GC–MS Analysis of TMS and Acetate Derivatives

One sample per food and hydrolysis procedure was analyzed for TMS derivatives and certain selected samples were analyzed for acetate derivatives by GC–MS on a Hewlett-Packard 6890 GC (Wilmington, PA, USA) equipped with an Agilent 5973 MS (Palo Alto, CA, USA). An S/SL injector was used; the injection volume varied from 0.2 to 1 μl. MSD interface temperature was 280 °C and ion source temperature was 230 °C; electron impact ionization was performed at 70 eV.

UPLC-QTOF/MS Analysis

As a complementary method for the identification of SG, of which the FS coelute in the GC method (spinasterol, poriferasta-7,22,25-trienol and sitosterol), non-hydrolyzed purified SG fractions from the foods of interest were analyzed by UPLC-QTOF/MS. Based on the different mass-to-charge ratio (*m/z*) of poriferasta-7,22,25-trienyl, spinasteryl and sitosteryl glucoside, their relative proportion

to each other was determined. Analyses were performed based on the method published in Oppliger et al. [37]. In short, separation of SG was performed using a methanol/water gradient on a reverse phase UPLC column (BEH C18, Waters, Milford, USA) in a ACQUITY Ultra-performance LC (UPLC) system (Waters, Milford, USA) interfaced to a QTOF-MS system (Synapt G2, Waters, Milford, USA). The detection of sodiated SG ions $[SG + Na]^+$ was performed in positive electrospray ionization mode. The complete results are in the supplementary material.

Data Evaluation

Chromatographic peaks in the GC-FID method were included in the integration if they appeared in each of the three chromatograms (triplicate samples) and were confirmed to be a sterol compound by GC–MS. The sterol peaks were evaluated on the basis of the relative retention time (RRT) to the IS in the GC-FID method after comparison of GC–MS and GC-FID chromatograms and identification of the peaks. The GC mass spectra were edited with OriginPro 8.5, and sterol relevant peaks were labeled. GC–MS spectra were evaluated based on mass-to-charge ratio (*m/z*) of the molecular ion and characteristic fragment ions. Identification of sterols was based on characteristic fragmentation patterns either from TMS or acetate derivatives [38], and on comparison to published spectral data on TMS-derivatives [23, 39, 40]. Poriferasta-7,25-dienol was identified based on the published GC–MS spectrum of stigmasta-7,25-dienol [40], and the fact that it is found as (24S)-epimer in *Cucurbitaceae* [31]. Sterols assigned as artifacts were compounds that only appeared after acid hydrolysis, and therefore, were formed during sample preparation.

Statistical analyses were performed using SPSS Statistics 17.0 for Windows (SPSS Inc, Chicago, USA). Independent samples *t* test was performed on triplicates (confidence interval = 95 %).

Results

Impact of Hydrolysis Procedure on Quantification and Sterol Profiles of SG

When comparing acid and enzymatic hydrolysis, the recovery of FS after the hydrolysis of the pure SG mixture consisting of Δ^5-steryl glucosides (200 µg) was substantially different. Complete hydrolysis would release 144 µg total FS. However, the acid hydrolysis procedure applied in this study, also including alkaline hydrolysis in order to remove saponifiable compounds originating from the addition of milk, resulted in a FS recovery of only 26.2 ± 5.1 %.

Table 1 Total steryl glycoside (SG) amount of lipid extracts from melon, pumpkin seeds, amaranth and beetroot when analyzed after enzymatic or acid hydrolysis (percentage difference compared to enzymatic hydrolysis in parentheses)

	Dry matter (g/100 g)	Total SG amount (µg/g DM)	
		Enzymatic hydrolysis	Acid hydrolysis
Melon	9.7	83.3 ± 16.2	29.6 ± 2.3 (64 %)
Pumpkin seeds	95.3	123.6 ± 19.0	74.9 ± 11.1 (40 %)
Amaranth	88.8	102.8 ± 22.7	31.5 ± 7.5 (69 %)
Beetroot	13.7	128.3 ± 0.6	30.8 ± 2.2 (76 %)

However, enzymatic hydrolysis resulted in a recovery rate of 83.1 ± 13.4 %. In an additional experiment using acid hydrolysis but without the addition of milk, the recovery rate was increased to 44.1 ± 0.3 % when compared to samples with the addition of milk. However, degradation products of the Δ^5-sterols were most likely formed at these conditions, demonstrated by three newly eluting peaks detected in the GC-FID chromatogram (see supplementary data Figure 1).

The total SG amounts of four foods dominated by Δ^7-sterols were compared by acid and enzymatic hydrolysis (Table 1). Similar to the Δ^5-steryl glucoside standard mixture, substantially lower values were observed after acid hydrolysis as compared to enzymatic hydrolysis. These amounts were up to 76 % lower, e.g., in case of total SG extracted from beetroot. In order to determine sterol composition of the SG fraction, we further focused on the proportion of single sterol species, rather than on content of single sterol species due to the evident dependency of the total SG content on the hydrolysis procedure.

The two different hydrolysis procedures had a drastic impact on the sterol species formed and detected by GC-FID for the foods rich in Δ^7-sterols (Fig. 2). Differences were found not only in sterol species, but also in numbers of sterols detected and peak sizes (in relation to IS), showing that resulting sterol profiles were not identical after acid and enzymatic hydrolysis. The most drastic difference was found for pumpkin seeds: the SG fraction consisted of a much higher number of sterols after acid hydrolysis than when mild enzymatic hydrolysis was performed.

Sterol Composition of SG of Selected Foods from *Cucurbitaceae* and *Amaranthaceae* after Enzymatic and Acid Hydrolysis

SG extracted from melon were used as an example to elucidate the origin of artifact sterols and the detection of labile SG. As shown by the overlay of the GC-chromatograms of melon SG hydrolyzed with either enzyme or acid, the
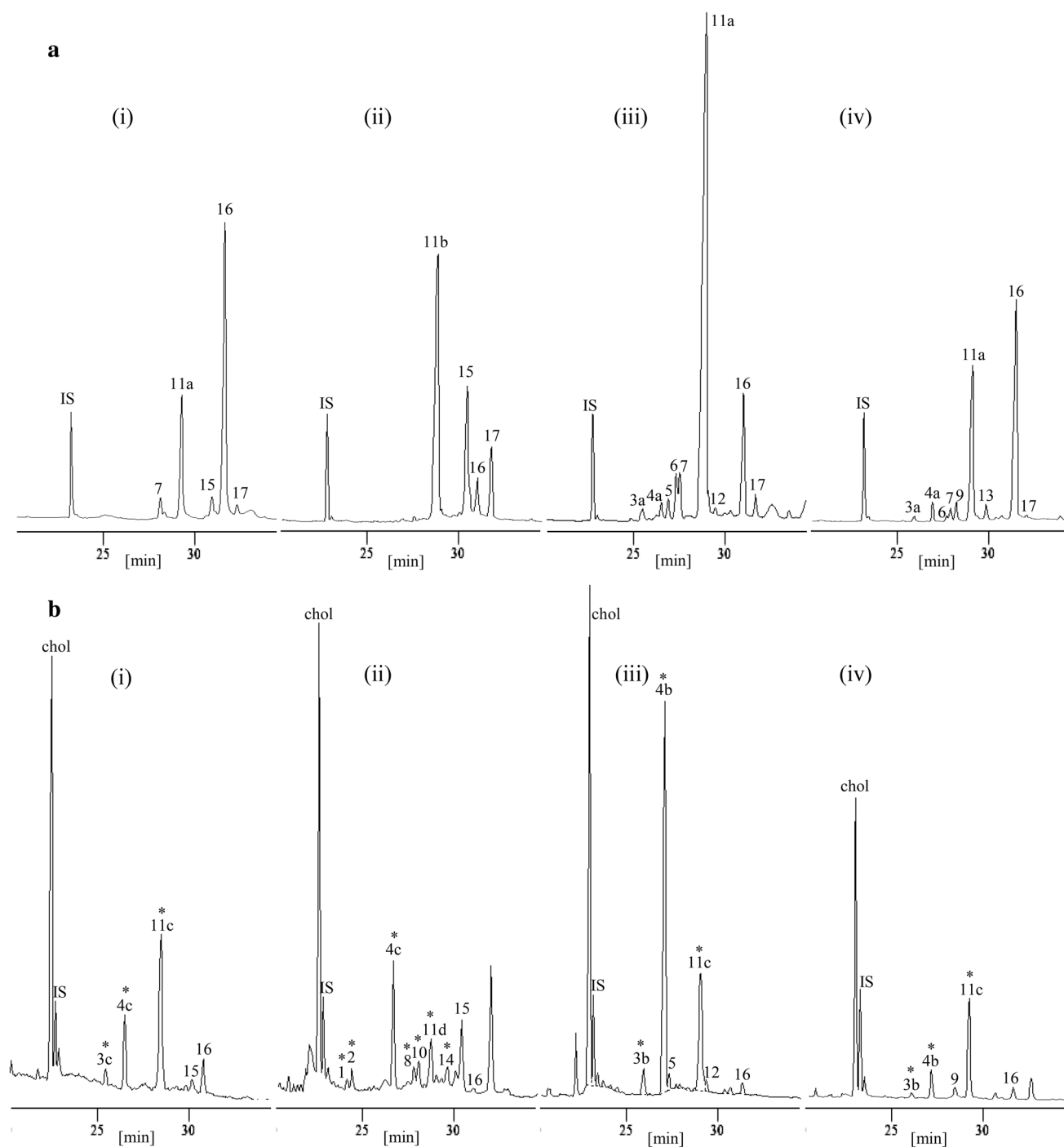
Fig. 2 GC-FID chromatograms of free sterols (FS) after **a** enzymatic hydrolysis and **b** acid hydrolysis of SG from melon (*i*), pumpkin seeds (*ii*), amaranth (*iii*) and beetroot (*iv*). Same peak numbers indicate sterols with same relative retention time (RRT) to internal standard (IS); *different letters* indicate different identity of sterols; peaks labeled with an *asterisk* (*) derive exclusively from artifact sterols or contain artifact sterol. *Chol* cholesterol derived from sample preparation. *1* Artifact of poriferasta-7,22,25-trienol; *2* artifact of poriferasta-7,22,25-trienol; *3a* campesterol; *3b* campesterol + artifact of Δ^7-campesterol; *3c* artifact of Δ^7-campesterol; *4a* stigmasterol; *4b* stigmasterol + artifact of spinasterol; *4c* artifact of spinasterol; *5* unidentified sterol *m/z* 486; *6* unidentified sterol *m/z* 484; *7* Δ^7-campesterol; *8* unidentified sterol *m/z* 484; *9* unidentified sterol *m/z* 486, *10* unidentified sterol *m/z* 484; *11a* spinasterol (+ sitosterol); *11b* spinasterol + poriferasta-7,22,25-trienol; *11c* spinasterol + artifact of Δ^7-stigmastenol; *11d* spinasterol, poriferasta-7,22,25-trienol + artifact of Δ^7-stigmastenol; *12* unidentified stanol *m/z* 488; *13* unidentified sterol *m/z* 486; *14* artifact of poriferasta-7,22,25-trienol; *15* poriferasta-7,25-dienol; *16* Δ^7-stigmastenol; *17* Δ^7-avenasterol

peak at RRT 1.25 did not reveal identical mass spectra after enzymatic and acid hydrolysis (Fig. 3b, f). After enzymatic hydrolysis, the sterol was identified as spinasterol (m/z 484), but after acid hydrolysis the molecular ion was m/z 486; an isomer of Δ^7-stigmastenol. The sterols that only appeared after acid hydrolysis were eluting prior to their original sterols (Fig. 3d, e). Their mass spectra showed that the molecular ion was m/z 472 (RRT 1.12) and m/z 484 (RRT 1.16) corresponding to the m/z of Δ^7-campesterol and spinasterol, respectively, thus being their artifact sterols.

When hydrolyzed enzymatically, five major sterols in the SG fraction of melon were identified (Table 2), with the highest proportion being identified as Δ^7-stigmastenol (66.0 %), followed by spinasterol (25.3 %). LC–MS analysis of the SG fraction also showed that poriferasta-7,22,25-trienyl glucoside occurred in melon, coeluting with spinasterol as FS during our GC method. Thus, the peak at RRT 1.25 was not pure spinasterol, but also contained poriferasta-7,22,25-trienol (~24 %), as is known for *Cucurbitaceae*. On the other hand, there is no sterol known that would coelute with Δ^7-stigmastenol (RRT 1.35). Furthermore, the occurrence of Δ^7-campesterol could be confirmed by GC–MS, which had a RRT of 1.21 in the GC-FID method and was 3.4 % of total SG. Δ^7-avenasterol was found at a percentage of 2.0 %.

After acid hydrolysis, the sterol with RRT 1.25, assigned as an artifact originating from Δ^7-stigmastenol, was most dominant (Table 2). Furthermore, the sterols with RRT 1.12 and RRT 1.16, assigned as the artifacts of Δ^7-campesterol and of Δ^7-stigmastenol, respectively, occurred only in the acid treated samples. We confirmed that these were not Δ^5-sterols due to the absence of an intense m/z 129 ion (characteristic to Δ^5-sterols) and the presence of m/z 255. In detail, the acid hydrolyzed SG fraction was highest in the artifact of Δ^7-stigmastenol (62.8 %), followed by the sterol with RRT 1.16 (artifact of spinasterol, 21.3 %), which almost corresponded to the original percentage of these sterols when enzymatic hydrolysis was performed. After acid hydrolysis, Δ^7-stigmastenol was not completely isomerized; 7.9 % of the original amount was found, which represents 87 % less than the Δ^7-stigmastenol observed following enzymatic hydrolysis. Alternatively, the percentage of poriferasta-7,25-dienol was almost the same as after enzymatic hydrolysis (3.3 %), and the artifact of Δ^7-campesterol was 3.3 %. The peak of Δ^7-avenasterol did not occur after acid hydrolysis, and its artifact must have coeluted with other sterols, but could not be identified by MS due to low abundance.

The analysis of the second *Cucurbitaceae* sample, pumpkin seeds (Table 2), showed that the SG fraction was dominated by spinasterol and poriferasta-7,22,25-trienol, both of which coeluted at RRT 1.25. LC–MS analysis

showed that around 55 % of the peak consisted of poriferasta-7,22,25-trienol, thus being the most abundant sterol in the SG fraction of pumpkin seeds. In GC–MS, poriferasta-7,22,25-trienol eluted slightly earlier than spinasterol, but they were not baseline separated. The fragment ion with m/z 343 confirmed that both sterols contained a double bond at C-22. Based on the integration of the peak of these coeluting sterols, the percentage of spinasterol/poriferasta-7,22,25-trienol was 63.6 %. As in melon SG, poriferasta-7,25-dienol (23.0 %), Δ^7-avenasterol (7.8 %) and Δ^7-stigmastenol (5.2 %) were found. However, the percentage of Δ^7-stigmastenol was significantly lower than in melon and Δ^7-campesterol was not detected.

Again, the composition of the SG fraction was completely different when acid hydrolysis was performed on pumpkin seeds SG, as shown by the drastic increase of number of peaks in the chromatogram. Only one peak was identical to the one from the enzymatically treated samples: poriferasta-7,25-dienol accounted for almost one quarter of the total SG. After acid hydrolysis, the peak of coeluting spinasterol/poriferasta-7,22,25-trienol, previously observed with enzymatic hydrolysis, now contained m/z 486 (artifact of Δ^7-stigmastenol) in addition to m/z 484 (spinasterol), but m/z 482 (poriferasta-7,22,25-trienol) could not be detected. Thus, spinasterol was not completely isomerized to another species and poriferasta-7,22,25-trienol (m/z 482) seemed to undergo isomerization to other sterol species as three new peaks appeared after acid hydrolysis at RRT 1.06, 1.07 and RRT 1.29, all with the dominant ion m/z 482. Moreover, two additional, almost coeluting artifact peaks appeared at RRT 1.21 and RRT 1.22 (peak 8 and 10 in Fig. 2); both were characterized by m/z 484 and are possible artifacts from poriferasta-7,25-dienol.

In contrast to the two *Cucurbitaceae* samples, Δ^5-sterols were identified in the two *Amaranthaceae* samples, which were characterized by an intense m/z 129 in the mass spectrum (Fig. 4a). However, the SG fraction extracted from amaranth seeds and enzymatically hydrolyzed was clearly dominated by spinasterol (73.7 %), followed by Δ^7-stigmastenol at a proportion of 11.9 % (Table 3). The other sterols occurred in minor proportions: Δ^7-campesterol (3.5 %), Δ^7-avenasterol (2.1 %), Δ^5-campesterol (1.4 %), and Δ^5-stigmasterol (0.9 %), along with three unidentifed sterols (peak 5, 6 and 12 in Fig. 2).

After acid hydrolysis the SG fraction of amaranth was highest in the sterol, which coeluted with Δ^5-stigmasterol and contained the artifact of spinasterol (60.5 %) (Table 3; Fig. 4b). The spinasterol peak observed after acid hydrolysis was dramatically smaller (25.9 %), as was that for Δ^7-stigmastenol (3.8 %). The peak of the sterol that was identified as Δ^5-campesterol was larger after acid hydrolysis (4.8 %), indicating a coeluting artifact sterol, which was confirmed by the MS spectrum.

Fig. 3 GC-FID chromatogram overlay and GC mass spectra for the most abundant sterols (as TMS derivatives) after enzymatic hydrolysis (**a–c**) and after acid hydrolysis (**d–f**) of steryl glycoside (SG) from melon; **a** relative retention time to internal standard (RRT) 1.21, Δ^7-campesterol; **b** RRT 1.25, spinasterol; **c** RRT 1.35, Δ^7-stigmastenol; **d** RRT 1.12, artifact of Δ^7-campesterol; **e** RRT 1.16, artifact of spinasterol and **f** RRT 1.25, artifact of Δ^7-stigmastenol
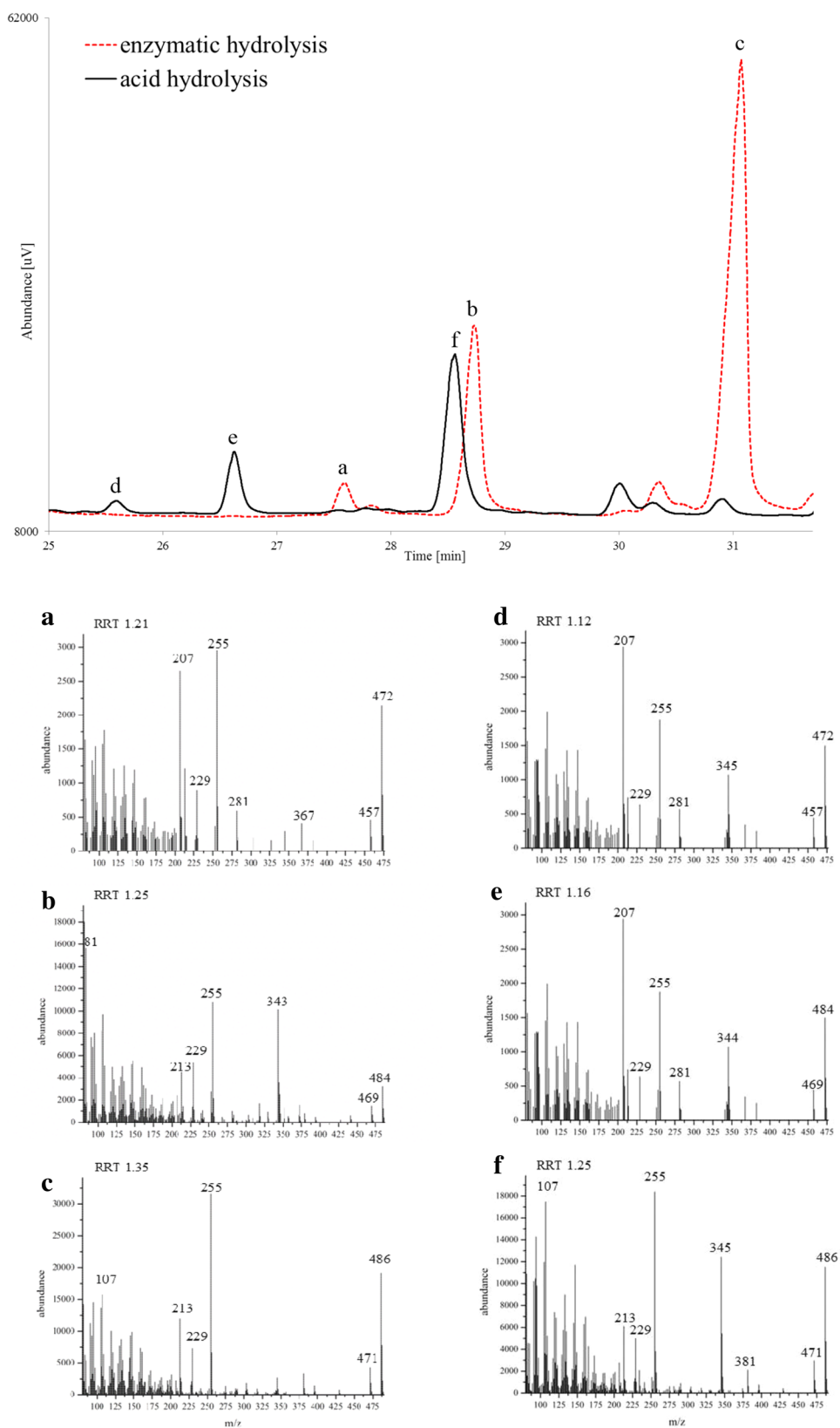
Table 2 Sterol composition [%] of steryl glycosides (SG) from melon and pumpkin seeds after acid and enzymatic hydrolysis and relative retention time to internal standard (RRT) of released free sterols (FS) as TMS derivatives; sterol numbering (No.) is based on order of appearance and is as used in Fig. 2

Sterol (artifact sterol) [%]	No.	RRT	Melon		Pumpkin seeds	
			Acid	Enzymatic	Acid	Enzymatic
(Artifact of poriferasta-7,22,25-trienol)	1	1.06			7.4 ± 1.8	
(Artifact of poriferasta-7,22,25-trienol)	2	1.07			5.0 ± 0.6	
(Artifact of Δ^7-campesterol)	3c	1.12	3.3 ± 1.5			
(Artifact of spinasterol)	4c	1.16	21.3 ± 0.5		33.9 ± 0.6	
(Artifact with *m/z* 484)	8	1.21			8.3 ± 0.3	
Δ^7-Campesterol	7			3.4 ± 0.3		
(Artifact with *m/z* 484)	10	1.22			6.2 ± 0.8	
Spinasterol + poriferasta-7,22,25-trienol[*] (+ sitosterol)	11b	1.25		25.3 ± 0.7		63.6 ± 2.6
(Artifact of Δ^7-stigmastenol) + spinasterol + poriferasta-7,22,25-trienol (+ sitosterol)	11d		62.8 ± 3.7		14.7 ± 1.3	
(Artifact of poriferasta-7,22,25-trienol)	14	1.29			1.8 ± 0.7	
Poriferasta-7,25-dienol	15	1.33	4.4 ± 0.4	3.3 ± 0.6	22.7 ± 0.1	23.0 ± 0.4
Δ^7-Stigmastenol	16	1.35	7.9 ± 2.9	66.0 ± 0.1		5.2 ± 0.5
Δ^7-Avenasterol	17	1.38		2.0 ± 0.4		7.8 ± 2.0

[*] Poriferasta-7,22,25-trienol coelutes with spinasterol in GC-FID method and presence has been confirmed by UPLC-QTOF/MS (see supplementary material)

Fig. 4 GC mass spectra of TMS-derivatives of the sterol at relative retention time to internal standard (RRT) 1.16; **a** after enzymatic hydrolysis (Δ^5-stigmasterol) and **b** after acid hydrolysis (Δ^5-stigmasterol and dominating, coeluting isomeric sterol, artifact of spinasterol) of SG from amaranth
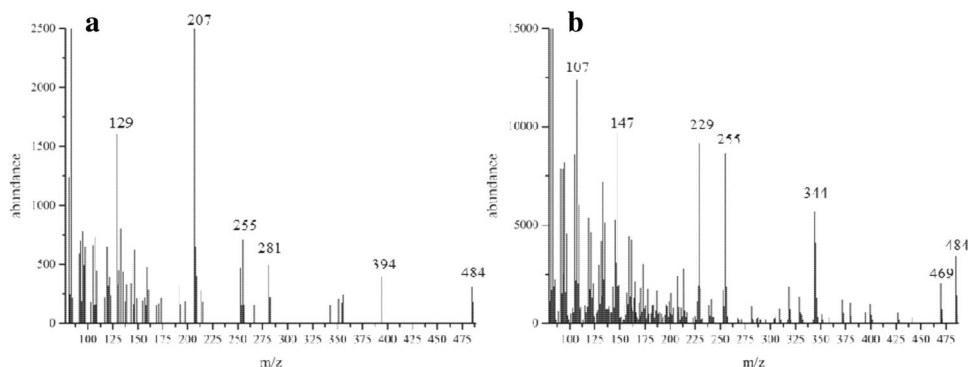
The SG fraction from beetroot was a complex mixture of at least 11 sterols, with some of them coeluting (Table 3). After enzymatic hydrolysis, the highest percentage was found for Δ^7-stigmastenol (51.7 %). Unlike in the other food samples, sitosterol was the dominant species in the peak at RRT 1.25, where it was coeluting with spinasterol (confirmed by UPLC-QTOF/MS, see supplementary material); together they made up 33.7 %. As with amaranth, two Δ^5-sterols were found: Δ^5-stigmasterol (3.2 %) and Δ^5-campesterol (0.9 %). Other sterols were Δ^7-campesterol (2.4 %), poriferasta-7,25-dienol (1.1 %), Δ^7-avenasterol, and three unidentified sterols (peak 6, 9 and 13 in Fig. 2). After acid hydrolysis, the proportion of the former sitosterol/spinasterol peak was remarkably larger at 63.9 %, due to the coelution of Δ^7-stigmastenol artifact. Simultaneously, the remaining non-isomerized Δ^7-stigmastenol was smaller at 8.1 %. A larger peak was observed for the RRT 1.16 consisting not only of Δ^5-stigmasterol but also of the artifact from spinasterol (18.0 %).

Identification of Artifact Sterols

Several different artifact sterols can be formed from Δ^7-sterols after the formation of tertiary carbenium ions (Fig. 5). In this study, the identification of the artifact peaks was based on GC–MS spectra from TMS and acetate derivatives. The comparison to MS spectra of the original sterols resulted in valuable information in addition to the RRT, which was crucial for reliable identification.

Substantial differences in the GC-spectra of the artifact sterols and their original Δ^7-sterols were observed. As a TMS derivative, Δ^7-stigmastenol yielded *m/z* 255 as a base

Table 3 Sterol composition [%] of steryl glycosides (SG) from amaranth and beetroot after acid and enzymatic hydrolysis and relative retention time to internal standard (RRT) of released free sterols as TMS derivatives; sterol numbering (No.) is based on order of appearance and used in Fig. 2

Sterol (artifact sterol) [%]	No.	RRT	Amaranth		Beetroot	
			Acid	Enzymatic	Acid	Enzymatic
Δ^5-Campesterol	3a	1.12		1.4 ± 0.2		0.9 ± 0.1
(Artifact of Δ^7-campesterol) + Δ^5-campesterol	3b		4.8 ± 0.2		3.3 ± 0.2	
Δ^5-Stigmasterol	4a	1.16		0.9 ± 0.4		3.2 ± 0.5
(Artifact from spinasterol) + Δ^5-stigmasterol	4b		60.5 ± 5.2		18.0 ± 1.4	
Unknown sterol with m/z 486	5	1.18	2.1 ± 0.2	2.1 ± 0.6		
Unknown sterol with m/z 484	6	1.20		3.2 ± 0.5		0.8 ± 0.1
Δ^7-Campesterol	7	1.21		3.5 ± 0.6		2.4 ± 0.2
Unknown sterol with m/z 486	9	1.22			5.7 ± 1.4	3.6 ± 0.3
Spinasterol (+ sitosterol)*	11a	1.25		73.7 ± 1.7		33.7 ± 0.4
(Artifact of Δ^7-stigmastenol) + spinasterol (+ sitosterol)	11c		25.9 ± 2.5		63.9 ± 0.3	
Stanol with m/z 488 (sitostanol)	12	1.26	2.0 ± 2.0	1.2 ± 0.3		0.5 ± 0.1
Unknown sterol with m/z 486	13	1.28				2.2 ± 0.2
Poriferasta-7,25-dienol†	15	1.33			1.1 ± 0.2	1.1 ± 0.3
Δ^7-Stigmastenol	16	1.35	3.8 ± 1.9	11.9 ± 1.7	8.1 ± 0.5	51.2 ± 0.2
Δ^7-Avenasterol	17	1.38		2.1 ± 0.4		0.5 ± 0.1

* Beetroot contained remarkable amount of sitosteryl glucoside (confirmed by UPLC-QTOF/MS, see supplementary material)

† Or possibly stigmasta-23(24)-dienol

peak (M-SC-ROH, facile loss of side chain and functional group is indicative for Δ^7-sterols), and an intense molecular ion characteristic for Δ^7-sterols (Fig. 3, spectrum c). The mass spectrum of the artifact sterol was different with regards to the appearance of m/z 345 (M-SC) (Fig. 3, spectrum f). The GC–MS spectrum of spinasterol was characterized by intense m/z 255 and 343 (M-SC, indicative for unsaturated SC in Δ^7-sterols) (Fig. 3, spectrum b). Its artifact sterol yielded m/z 344, higher than m/z 343 (Fig. 3, spectrum e). Δ^7-campesterol yielded m/z 255 as a characteristic peak and an intense molecular ion (Fig. 3, spectrum a). For its artifact sterol, an additional ion with m/z 345 (M-SC) was formed (Fig. 3, spectrum d).

The artifact peaks of Δ^7-campesterol, spinasterol, and Δ^7-stigmastenol were also analyzed by GC–MS as acetate derivatives. In the three spectra (Fig. 6), M^+ appeared and m/z 255 (M-SC) was predominant. Also, m/z 229 (M-SC-ROH-26) was formed from these three artifact sterols. Other typical ions were m/z 315 and 382 for the Δ^7-campesterol artifact, m/z 314 (M-ROH) for the spinasterol artifact, and m/z 315 (M-ROH) and 441 (M–Me) for the Δ^7-stigmastenol artifact.

As TMS and acetate derivatives, the artifacts of the Δ^7-sterols were eluting at the same RRT as their corresponding Δ^5-sterol variants. For instance, the spinasterol artifact as an acetate derivative had a RRT 1.18, which was identical to the RRT of Δ^5-stigmasterol standard as an acetate derivative. As mentioned above, the SG fraction from amaranth contained Δ^5-stigmasterol and Δ^5-campesterol, which were masked by their isomeric artifacts from Δ^7-sterols after acid hydrolysis was performed.

Discussion

The recovery of FS after the hydrolysis of the standard mixture consisting of Δ^5-sterols was significantly affected by the choice of the hydrolysis procedure. In the case of acid hydrolysis with the addition of milk in order to mimic food matrix, the values were extremely low, suggesting either insufficient hydrolysis or impaired extractability. On the other hand, if the milk addition was omitted, higher recovery could be achieved, but simultaneously degradation products were detected as three new peaks occurred in the GC-FID chromatogram (supplementary data Figure 1). Sterols might not only be sensitive towards isomerization at low pH and high temperature, but released FS may also undergo dehydration reactions under highly acidic conditions. A decomposition of 80 % was previously demonstrated on FS from oats, even though the acid hydrolysis performed included the potentially protective food matrix [41]. Acid-catalyzed dehydration of free sterols resulting in 3,5-diene has been demonstrated for Δ^5-sterols [42]. The possibility of thermoxidation due to presence of C=C double bonds which was characterized by different susceptibility of Δ^5- and Δ^7-sterols has also been suggested [43]. The

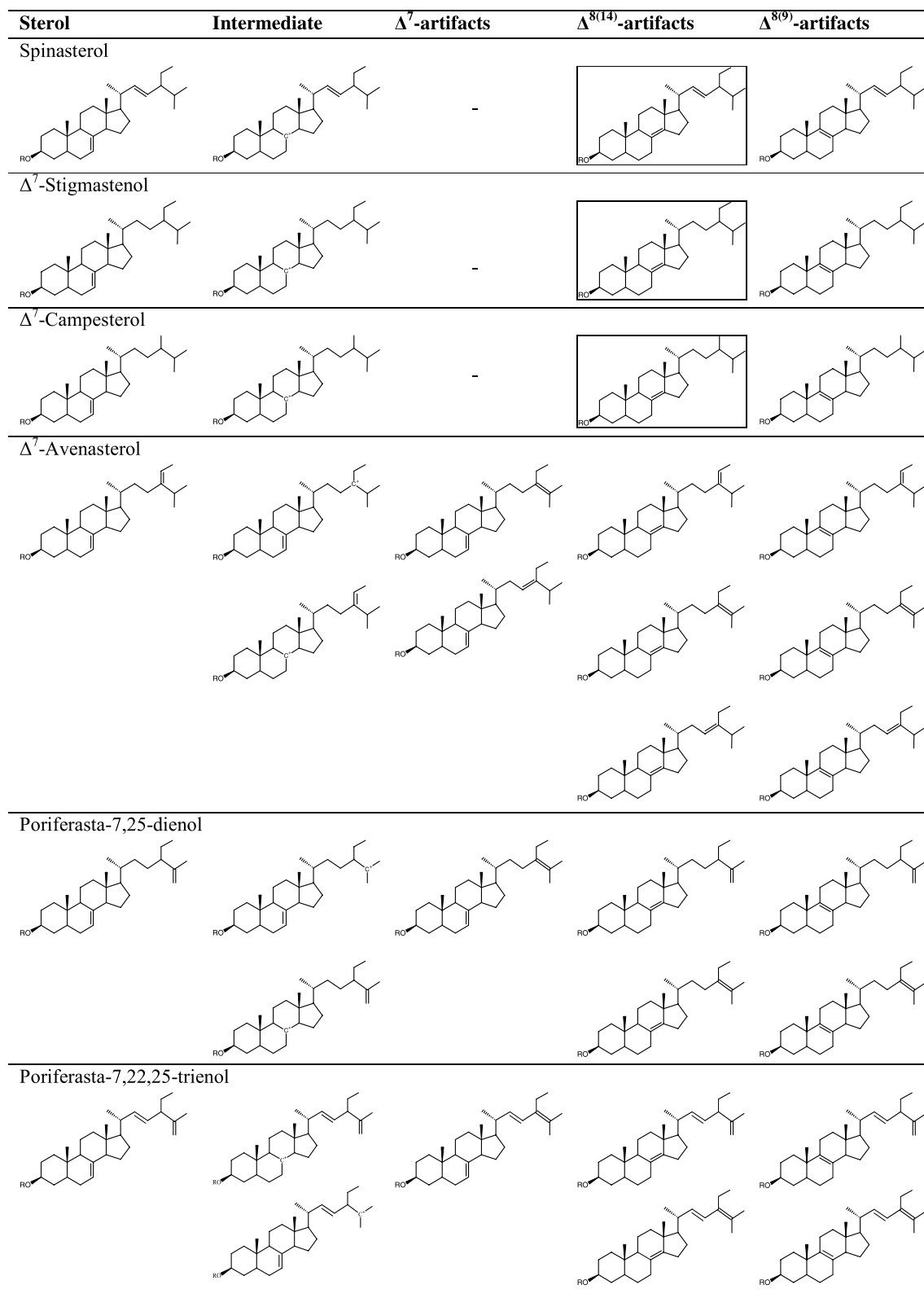| Sterol	Intermediate	Δ^7-artifacts	$\Delta^{8(14)}$-artifacts	$\Delta^{8(9)}$-artifacts
Spinasterol		-		
Δ^7-Stigmastenol		-		
Δ^7-Campesterol		-		
Δ^7-Avenasterol				
Poriferasta-7,25-dienol				
Poriferasta-7,22,25-trienol				

Fig. 5 Tertiary carbenium ions (intermediates) and possible isomerization products (artifacts) of Δ^7-sterols formed under acidic conditions; encircled sterols were identified in this study ($\Delta^{8(14)}$-sterols), *R* glycosidic residue as steryl glycoside or H as free sterol
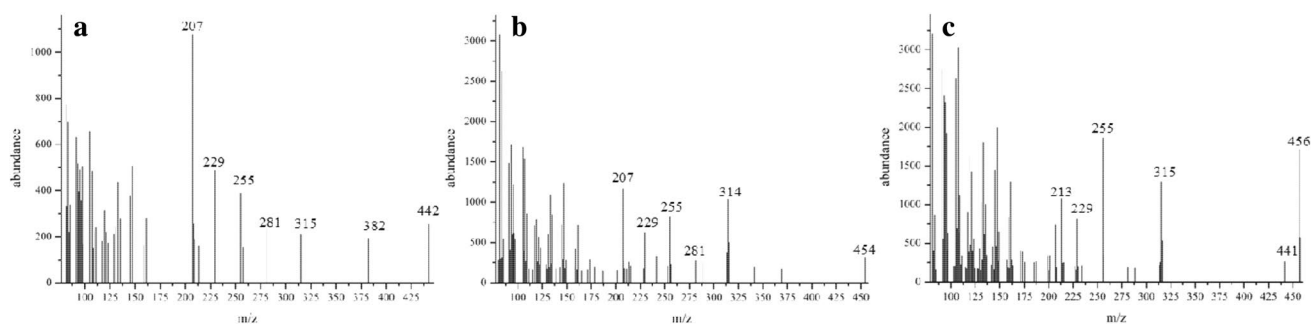
Springer AOCS

Fig. 6 GC-MS spectra of acetate derivatives of **a** $\Delta^{8(14)}$-campesterol (artifact of Δ^7-campesterol, amaranth), **b** stigmasta-8(14),22-dienol (artifact of spinasterol, melon), and **c** $\Delta^{8(14)}$-stigmastenol (artifact of Δ^7-stigmastenol, melon), detected only after acid hydrolysis

results of the current study point out that it is highly difficult to perform acid hydrolysis achieving full conversion of SG into FS, as it is a balance between sufficient hydrolysis and avoiding sterol degradation. These data demonstrate again the importance of an alternative procedure; for instance, enzymatic hydrolysis, which provided much higher recovery and, in addition, avoided isomerization.

The hydrolysis of SG extracted from foods dominated by Δ^7-sterols showed that these are highly labile sterols, which has also been demonstrated by other studies [17, 23, 27, 28]. For instance, Phillips et al. [23] showed that Δ^7-stigmastenol only appeared if sterols from pumpkin seeds were not subjected to acid hydrolysis. They published the GC–MS spectrum of a sterol with m/z 484 that only appeared after acid hydrolysis, and which had an identical retention time as Δ^5-stigmasterol; however, the identity of this sterol was not assessed. No further analyses determining the correct percentage of those sterols could be performed, due to the lack of mild hydrolysis [23]. In an earlier work by our laboratory, the artifact sterols of Δ^7-sterols (one coeluting with stigmasterol and one coeluting with spinasterol) were tentatively assigned as Δ^8-sterols based on GC–MS data, but the isomerization pathway could not yet be determined [17]. In the present study, based on data gathered after enzymatic hydrolysis, we were able to identify the highly labile sterols, namely spinasterol, Δ^7-stigmastenol, Δ^7-campesterol and poriferasta-7,22,25-trienol, and we were able to assign and characterize their artifact peaks generated in the acid hydrolysis. We showed that Δ^7-stigmastenol was highly sensitive to isomerization. Therefore, not only are sterols with an alkene side chain susceptible to isomerization, but isomerization also occurs at other places in the molecule. In this case, the double bond at C-7 must be highly prone to forming a carbenium ion at low pH, resulting in the formation of isomer species. Resulting isomers of Δ^7-stigmastenol would either be $\Delta^{8(9)}$-stigmastenol or $\Delta^{8(14)}$-stigmastenol (Fig. 5). However, no diagnostic fragment ions exist for Δ^8-sterols, when compared to Δ^7-sterols as TMS-derivatives. Δ^8-Sterols

also show strong molecular ion and predominant m/z 255, both of which were found in the mass spectra of the artifact peaks. Differentiation of Δ^8-sterols from Δ^7-sterols can only be performed by comparison of their retention times [38]. The identified artifact peaks eluted earlier than their assigned original sterols. For example, in the case of amaranth, we showed that the isomers of the Δ^7-sterols that were formed had identical retention times as their respective Δ^5-sterols. Gerst et al. [44] showed that $\Delta^{8(14)}$-sterols coelute with their Δ^5-sterols as acetate and as TMS derivatives, most likely suggesting that Δ^7-sterols are transformed into $\Delta^{8(14)}$-sterols under acidic conditions. Transformation of Δ^7-sterols into $\Delta^{8(14)}$-sterols has been observed upon bleaching during oil refining [45]. Thus, the artifact peaks of spinasterol, Δ^7-stigmastenol, Δ^7-campesterol, and poriferasta-7,22,25-trienol observed in this study were stigmasta-8(14),22-dienol, $\Delta^{8(14)}$-stigmastenol, $\Delta^{8(14)}$-campesterol, and poriferasta-8(14),22,25-trienol, respectively. As TMS derivatives, difference in the mass spectrum of the artifact sterol was in the appearance of the ion, which is caused by the loss of the side chain that is only yielded for Δ^7-sterols if a double bond at C-22 is present. Therefore, the artifact sterols are more prone to the loss of their side chain than their Δ^7-sterols. As acetate derivatives, and the spectra were characterized by the dominant appearance of m/z 229 (M-SC-ROH-26), which has been shown to be a characteristic m/z for $\Delta^{8(14)}$-sterols [46].

After the protonation of C-8 under acidic conditions leading to the production of a tertiary carbenium ion (Fig. 5), it is thermodynamically more favorable that Δ^8-sterols are formed than Δ^7-sterols, due to the formation of a tetra-substituted double bond after deprotonation. However, why $\Delta^{8(14)}$-sterols are more likely to be produced cannot be easily explained in this context. In the case of Δ^7-avenasteryl, poriferasta-7,25-dienyl, and poriferasta-7,22,25-dienyl glycoside, even multiple artifact sterols could possibly be formed due to the presence of two sites for protonation. Those artifact sterols with a tetra-substituted double bond in side chain ($\Delta^{24(25)}$) and those with

tetra-substituted double bonds in the ring system ($\Delta^{8(14)}$ and $\Delta^{8(9)}$) would most likely be favored due to stability reasons. These multiple artifact sterols explain why GC chromatograms are more substantially different after acid hydrolysis than after enzymatic hydrolysis if high amounts of, for example, poriferasta-7,22,25-trienyl or poriferasta-7,25-dienyl glycoside are present, as was observed with pumpkin seeds.

Due to the fact that isomerized sterol species coeluted with other sterols and based on the observation that labile sterols did not fully isomerize to other species, acid hydrolysis is not an appropriate method for the determination of sterols in SG fractions from Δ^7-sterols dominated foods. Similarly, if Δ^7-sterols coexist with Δ^5-sterols, as for instance was found in the two *Amaranthaceae* samples, the proportion of the Δ^5-sterols also cannot be precisely determined. Therefore, only enzymatic hydrolysis is a reliable tool to determine accurate composition of SG extracts from a broad range of foods if the cleavage of the glycosidic bond is required. So far, sterols in plant foods rich in spinasterol and Δ^7-stigmastenol have not been accurately analyzed since the artifact sterol of Δ^7-stigmastenol coelutes with spinasterol, and it has been included in the amount of spinasterol. Also, acid hydrolysis has caused a drastic underestimation of Δ^7-stigmastenol; so far, the occurrence of Δ^7-stigmastenol as the most abundant sterol of the SG fraction of melon and beetroot has been overlooked.

The importance of the correct determination of Δ^7-sterol of plants is also demonstrated by the prominent role of pumpkin seed oil in the treatment of benign prostate hyperplasia [31]. Furthermore, it has been shown that spinasteryl glucoside can be used as a potential anti-inflammatory agent and protects fibroblast cells from adverse effects of UV radiation [47, 48], which emphasizes the therapeutic use of certain SG species for which potential sources have to be identified. Enzymatic hydrolysis allows improved sample preparation for the analysis of sterols in a broad range of plant materials due to the preservation of labile sterols and avoidance of artifact formation, as well as enabling the analysis of sterol profiles consisting of less abundant SG. Furthermore, it allows proper determination of daily intakes of total sterols and of specific sterol species, which are not only based on sitosterol, campesterol, stigmasterol, and their stanols, but also include Δ^7-sterols, which are dominant in plants such as from the family of *Cucurbitaceae* and *Amaranthaceae*, and which are important components of diets worldwide.

References

1. Moreau RA, Whitaker BD, Hicks KB (2002) Phytosterols, phytostanols, and their conjugates in foods: structural diversity, quantitative analysis, and health-promoting uses. Progr Lipid Res 41:457–500
2. Klingberg S, Ellegard L, Johansson I, Hallmans G, Weinehall L, Andersson H, Winkvist A (2008) Inverse relation between dietary intake of naturally occurring plant sterols and serum cholesterol in Northern Sweden. Am J Clin Nutr 87:993–1001
3. Ostlund RE, Racette SB, Okeke A, Stenson WF (2002) Phytosterols that are naturally present in commercial corn oil significantly reduce cholesterol absorption in humans. Am J Clin Nutr 75:1000–1004
4. De Smet E, Mensink RP, Plat J (2012) Effects of plant sterols and stanols on intestinal cholesterol metabolism: suggested mechanisms from past to present. Mol Nutr Food Res 56:1058–1072
5. European Food Safety Authority (2010) Scientific opinion on the substantiation of health claims related to plant sterols and plant stanols and maintenance of normal blood cholesterol concentrations (Id 549, 550, 567, 713, 1234, 1235,1466, 1634, 1984, 2909, 3140), and maintenance of normal prostate size and normal urination (Id 714, 1467, 1635) pursuant to article 13(1) of Regulation (Ec) No 1924/2006[1]. EFSA J 8:1813–1836
6. Food and Drug Administration (2010) Proposed rules: Food labeling; health claim; phytosterols and risk of coronary heart disease December 8. Federal Register 75. http://www.gpo.gov/fdsys/pkg/FR-2010-12-08/html/2010-30386.htm
7. Tateo M, Yoshikawa M, Takeuchi H, Fujii S, Mizobuchi H, Takeuchi H (1994) Effects of sterylglycosides from soybean on lipid indexes in the plasma, liver, and feces of rats. Biosci Biotech Bioch 58:494–497
8. Lin XB, Ma LN, Moreau RA, Ostlund RE (2011) Glycosidic bond cleavage is not required for phytosteryl glycoside-induced reduction of cholesterol absorption in mice. Lipids 46:701–708
9. Bouic PJD, Etsebeth S, Liebenberg RW, Albrecht CF, Pegel K, VanJaarsveld PP (1996) Beta-Sitosterol and beta-sitosterol glucoside stimulate human peripheral blood lymphocyte proliferation: implications for their use as an immunomodulatory vitamin combination. Int J Immunopharm 18:693–700
10. Yang G, An HJ (2014) Beta-sitosteryl-3-O-beta-glucopyranoside isolated from the bark of *Sorbus commixta* ameliorates proinflammatory mediators in raw 264.7 macrophages. Immunopharm Immunot 36:70–77
11. Pegel KH (1997) The importance of sitosterol and sitosterolin in human and animal nutrition. S Afr J Sci 93:263–268
12. Ling WH, Jones PJH (1995) Dietary phytosterols—a review of metabolism, benefits and side-Effects. Life Sci 57:195–206
13. Fernandez C, Suarez Y, Ferruelo AJ, Gomez-Coronado D, Lasuncion MA (2002) Inhibition of cholesterol biosynthesis by delta(22)-unsaturated phytosterols via competitive inhibition of sterol delta(22)-reductase in mammalian cells. Biochem J 366:109–119
14. Jonker D, Glatz JFC, Homan C, Posthumus MA, Vanderhoek GD, Katan MB (1985) Combined determination of free, esterified and glycosilated plant sterols in foods. Nutr Rep Int 32:943–951
15. Lampi AM, Piironen V, Toivo J (2004) Analysis of Phytosterols in Foods. In: Dutta PC (ed) Phytosterols as functional food components and nutraceuticals. Marcel Dekker Inc, New York
16. Lagarda MJ, Garcia-Llatas G, Farre R (2006) Analysis of phytosterols in foods. J Pharm Biomed Anal 41:1486–1496
17. Nyström L, Schär A, Lampi AM (2012) Steryl glycosides and acylated steryl glycosides in plant foods reflect unique sterol patterns. Eur J Lipid Sci Tech 114:656–669

18. Phillips KM, Ruggio DM, Ashraf-Khorassani M (2005) Analysis of steryl glucosides in foods and dietary supplements by solid-phase extraction and gas chromatography. J Food Lipids 12:124–140

19. Gomez-Coca RB, Perez-Camino MD, Moreda W (2012) Specific procedure for analysing steryl glucosides in olive oil. Eur J Lipid Sci Tech 114:1417–1426

20. del Rio JC, Prinsen P, Gutierrez A (2013) A comprehensive characterization of lipids in wheat straw. J Agr Food Chem 61:1904–1913

21. Prinsen P, Gutierrez A, Faulds CB, del Rio JC (2014) Comprehensive study of valuable lipophilic phytochemicals in wheat bran. J Agr Food Chem 62:1664–1673

22. Valsta LM, Lemstrom A, Ovaskainen ML, Lampi AM, Toivo J, Korhonen T, Piironen V (2004) estimation of plant sterol and cholesterol intake in Finland: quality of new values and their effect on intake. Brit J Nutr 92:671–678

23. Phillips KM, Ruggio DM, Ashraf-Khorassani M (2005) Phytosterol composition of nuts and seeds commonly consumed in the United States. J Agr Food Chem 53:9436–9445

24. Piironen V, Toivo J, Lampi A-M (2000) Natural sources of dietary plant sterols. J Food Comp Anal 13:619–624

25. Normen L, Johnsson M, Andersson H, van Gameren Y, Dutta P (1999) Plant sterols in vegetables and fruits commonly consumed in Sweden. Eur J Nutr 38:84–89

26. Kamal-Eldin A, Määttä K, Toivo J, Lampi AM, Piironen V (1998) Acid-catalyzed isomerization of fucosterol and delta(5)-avenasterol. Lipids 33:1073–1077

27. Kesselmeier J, Eichenberger W, Urban B (1985) High-performance liquid-chromatography of molecular species from free sterols and sterylglycosides isolated from oat leaves and seeds. Plant Cell Physiol 26:463–471

28. Breinhölder P, Mosca L, Lindner W (2002) Concept of sequential analysis of free and conjugated phytosterols in different plant matrices. J Chromatogr B 777:67–82

29. Xu S, Patterson GW, Schmid K (1986) Sterols of *Amaranthaceae*. Phytochemistry 25:1883–1886

30. Akihisa T, Ghosh P, Thakur S, Rosenstein FU, Matsumoto T (1986) Sterol compositions of seeds and mature plants of family *Cucurbitaceae*. J Am Oil Chem Soc 63:653–658

31. Strobl M (2004) Δ7-Sterole und Δ7-Sterolglykoside aus Samen von *Curcurbita Pepo* L.: Isolierung und Strukturaufklärung. Doctoral dissertation, Ludwig-Maximilians-Universität München

32. Akihisa T, Thakur S, Rosenstein FU, Matsumoto T (1986) Sterols of *Cucurbitaceae*—the Configurations at C-24 of 24-Alkyldelta-5-sterols, delta-7-sterols and delta-8-sterOLs. Lipids 21:39–47

33. Rodriguez JB, Gros EG, Bertoni MH, Cattaneo P (1996) The sterols of *Cucurbita moschata* ("Calabacita") seed Oil. Lipids 31:1205–1208

34. Itoh T, Tamura T, Matsumot T (1974) Sterols, methylsterols, and triterpene alcohols in 3 *Theaceae* and some other vegetable oils. Lipids 9:173–184

35. Fernández-Cuesta A, Jan CC, Fernández-Martínez JM, Velasco L (2014) Variability for seed phytosterols in sunflower germplasm. Crop Sci 54:190–197

36. Münger LH, Nyström L (2014) Enzymatic hydrolysis of steryl glycosides for their analysis in foods. Food Chem 163:202–211

37. Oppliger SR, Münger LH, Nyström L (2014) Rapid and highly accurate detection of steryl glycosides by ultraperformance liquid chromatography-quadrupole time-of-flight mass spectrometry (UPLC-Q-TOF-MS). J Agric Food Chem 62:9410–9419

38. Goad LJ, Akihisa T (1997) Mass Spectrometry of Sterols. Analysis of Sterols, Blackie Academic & Professional, London

39. Zhang X, Cambrai A, Miesch M, Roussi S, Raul F, Aoude-Werner D, Marchioni E (2006) Separation of delta 5- and delta 7-phytosterols by adsorption chromatography and semipreparative reversed phase high-performance liquid chromatography for quantitative analysis of phytosterols in foods. J Agric Food Chem 54:1196–1202

40. Mandl A, Reich G, Lindner W (1999) Detection of adulteration of pumpkin seed oil by analysis of content and composition of specific delta 7-phytosterols. Eur Food Res Tech 209:400–406

41. Kesselmeier J, Eichenberger W, Urban B (1984) Application of high performance liquid chromatography to analysis of free sterols, sterylglycosides and acylsterylglycosides. In: Siegenthaler PW (ed) Structure, Function and Metabolism of Plant Lipids, Elsevier Science Pubilshers B.V, Amsterdam

42. Patel MS, Peal WJ (1964) Acid-catalysed dehydration of 3-hydroxysteroids—II. Tetrahedron 20:2499–2510

43. Lengyel J, Rimarcik J, Vaganek A, Fedor J, Lukes V, Klein E (2012) Oxidation of sterols: energetics of C-H and O-H bond cleavage. Food Chem 133:1435–1440

44. Gerst N, Ruan BF, Pang JH, Wilson WK, Schroepfer GJ (1997) An updated look at the analysis of unsaturated C-27 sterols by gas chromatography and mass spectrometry. J Lipid Res 38:1685–1701

45. Biedermann M, Grob K, Mariani C, Schmidt JP (1996) Detection of desterolized sunflower oil in olive oil through isomerized delta-7-sterols. Z Lebensm Unters Forsch 202:199–204

46. Bouvier P, Rohmer M, Benveniste P, Ourisson G (1976) Delta 8(14)-Steroids in bacterium *Methylococcus capsulatus*. Biochem J 159:267–271

47. Lee TH, Jung M, Bang MH, Chung DK, Kim J (2012) Inhibitory effects of a spinasterol glycoside on lipopolysaccharide-induced production of nitric oxide and proinflammatory cytokines via down-regulating map kinase pathways and NF-Kappa B activation in Raw264.7 macrophage cells. Int Immunopharmacol 13:264–270

48. Lee TH, Lee SM, Lee DY, Son Y, Chung DK, Baek NI, Kim J (2011) A glycosidic spinasterol from *Koreana Stewartia* Promotes procollagen production and inhibits matrix metalloproteinase-1 expression in UVB-irradiated human dermal fibroblasts. Biol Pharm Bull 34:768–773